EUROPEAN ORGANIZATION FOR NUCLEAR RESEARCH

Proposal to the ISOLDE and Neutron Time-of-Flight Committee

# Transition probabilities of low-lying excited states in $^{210}$Po and $^{210}$Pb

September 2022

G. Georgiev[1], G. Rainovski[2], A.E. Stuchbery[3], Zs. Podolyák[4], A. Andreyev[5], D.L. Balabanski[6], A. Blazhev[7], F. Browne[8], F. Dunkel[7], L.M. Fraile[9], L. Gaffney[10], K. Gladnishki[2], J. Jolie[7], T. Kibedi[3], D. Kocheva[2], A. Kusoglu[6,13], G. J. Lane[3], J. Ljungvall[1], V. Manov[2], AJ Mitchel[3], N. Pietralla[11], M. Scheck[12], M. Stoyanova[2], K. Stoychev[1], N. Warr[7], V. Werner[11]

1 IJCLab, Orsay, France
2 Faculty of Physics, St. Kliment Ohridski, University of Sofia, Bulgaria
3 The Australian National University, Canberra, Australia
4 University of Surrey, Guildford, UK
5 University of York, York, UK
6 ELI-NP, IFIN, Bucharest, Romania
7 IKP, University of Cologne, Germany
8 ISOLDE, CERN, Geneva, Switzerland
9 Universidad Complutense, Madrid, Spain
10 University of Liverpool, Liverpool, UK
11 TU Darmstadt, Darmstadt, Germany
12 University of the West of Scotland, Paisley, UK
13 University of Istanbul, Istanbul, Turkey

Spokesperson(s): G. Georgiev (georgi.georgiev@ijclab.in2p3.fr), G. Rainovski (rig@phys.uni-sofia.bg), Zs. Podolyák (z.podolyak@surrey.ac.uk) and A.E. Stuchbery (Andrew.Stuchbery@anu.edu.au)
Local contact: F. Browne (Frank.Browne@cern.ch)

CERN-INTC-2022-036 / INTC-P-638
27/09/2022

## Abstract

We propose to perform Coulomb excitation of the very-long lived isotopes $^{210}$Po and $^{210}$Pb in off-line mode to study transition probabilities of the first $2^+$ excited states. $^{210}$Po ($t_{1/2}$ = 138 d) and $^{210}$Pb ($t_{1/2}$ = 22 y) have two protons or two neutrons, respectively, away from the doubly magic $^{208}$Pb. The structure of these isotopes has been studied for many years, however, the long-lived $6^+$ and $8^+$ states have hampered obtaining reliable information on the lifetimes for the lowest-lying excited states. The possibility of Coulomb exciting these states, using radioactive ion beams, provides a unique opportunity for ***understanding the behaviour of the seniority-2 configurations in $^{210}$Pb and $^{210}$Po*** which are the foundation for understanding the structure of the low-lying states of nuclei in the vicinity of $^{208}$Pb.

**Requested shifts: 9 shifts**
**Beamline: MINIBALL + CD-only**

## Physics case

The Nuclear Shell Model represents the most fundamental concept in nuclear structure physics. It naturally leads to the appearance of magic numbers due to existence of large energy gaps which are defined primarily by the shape of the potential and the spin-orbit interaction [Goep50]. Besides many other insights on the structure of nuclei, the shell model, in combination with pairing correlations, provides insights into the low-energy spectra of semi-magic nuclei. Low-energy excited states with J > 0 in semi-magic nuclei, with two or more particles in a single high-*j* shell, are formed by angular momentum recoupling of unpaired nucleons, forming multiplets of states that have one and the same number of unpaired nucleons. This number is called seniority (ν) [Shal63, Talm71] and can be considered as a good quantum number. In fact, the generalized seniority scheme [Talm71] represents a truncation of the nuclear shell model.

Among the semi-magic nuclei, ones having only two-valence particles play an important role. These nuclei serve as reference points, providing the properties of the basic $j^2$ configurations such as the energies of states with ν = 2 and the absolute *E*2 transition strengths for the seniority-changing transition (Δν = 2) $2^+_1 \rightarrow 0^+_1$ and the seniority-preserving transitions (Δν = 0) within the ν = 2 multiplet [Talm71]. Moreover, the *E*2 observables can be used for basic tests of complete shell-model calculations. This is of importance since it is the first step towards the shell model description of open shell nuclei. It can be expected that the features of the seniority scheme persist in open shell nuclei close to magic numbers in which low-energy excitations are dominated by one kind of nucleons up to the point where the *p-n* interaction becomes strong enough to trigger collective behaviour. In this respect, ***understanding the low-energy spectra of semi-magic nuclei, especially of those with only two valence particles, defines the foundation for the shell model description of open shell nuclei.***

The semi-magic nuclei $^{210}$Po and $^{210}$Pb, respectively, have two valence protons and two valence neutrons with respect to the doubly magic nucleus $^{208}$Pb. The energies of their yrast $2^+$, $4^+$, $6^+$, and $8^+$ states follow seniority-like patterns of decreasing energy splitting between adjacent states with increasing spin (cf. Fig. 1). These patterns suggest that the yrast states of $^{210}$Po belong to the $(\pi h_{9/2})^2$ multiplet while the ones of $^{210}$Pb belong to the $(\nu g_{9/2})^2$ multiplet. In the case of $^{210}$Po this assignment is strongly supported by large-scale shell-model calculations using realistic interactions [Cor99, Caur03]. Data on absolute strengths for *E*2 transitions between these states of both nuclei are also available [Häus76, Elleg73, Elleg71]. For $^{210}$Po the agreement of these data with the calculations [Cor99, Caur03] is very good except the fact that the calculated $B(E2;2^+_1 \rightarrow 0^+_1)$ transition strength ***overestimates the experimental value by a factor of six***. This discrepancy casts doubts on the first experimental $B(E2;2^+_1 \rightarrow 0^+_1)$ values in $^{210}$Po [Cor99, Caur03] and $^{210}$Pb both of which were deduced from experiments on inelastic scattering of deuterons, protons and tritons [Elleg73, Elleg71]. Motivated by the discrepancy between the adopted experimental value for the $B(E2;2^+_1 \rightarrow 0^+_1)$ [Sham14] in $^{210}$Po and the calculated one, Kocheva *et al.* [Koch17a] have remeasured the lifetime of the $2^+_1$ state of $^{210}$Po by employing the DSA method in a transfer reaction. The lifetime obtained in this measurement is 2.6(4) ps yielding an *E*2 transition strength of 136(21) $e^2fm^4$. ***Although this value tempers the discrepancy between theory and experiment there remains a factor of two difference – a significant disagreement for notably "simple" states***.

To demonstrate the discrepancy discussed above, in Fig. 1 we compare the experimental properties of the yrast states of $^{210}$Pb and $^{210}$Po to realistic shell-model calculations. The calculations were performed [Koch17b] in a valence space consisting of all neutron orbitals in the 126-184 shell ($3s_{1/2}$, $2d_{3/2}$, $2d_{5/2}$, $1g_{7/2}$, $1g_{9/2}$, $0h_{11/2}$, and $0j_{15/2}$) and all proton orbitals

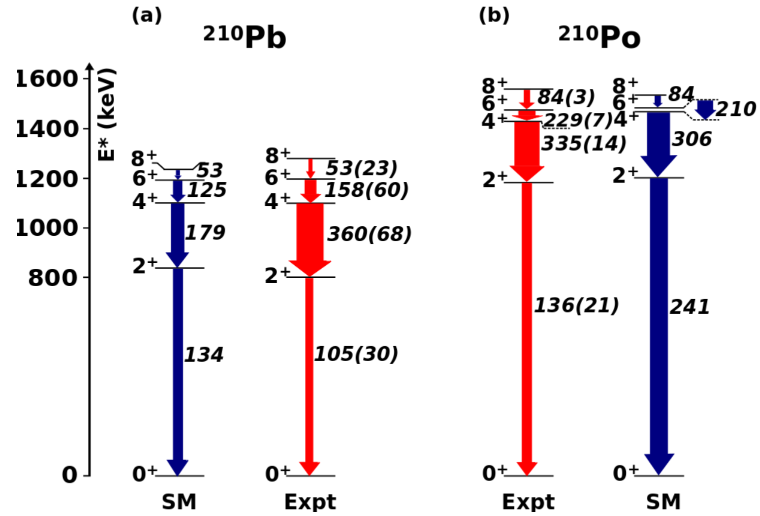


Figure 1: A graphical comparison between calculated (SM) and the experimental (Expt) properties of the yrast states in $^{210}$Pb (a) and $^{210}$Po(b). The thickness of the arrows is proportional to the B(E2) values. The latter are also presented by the numbers next to the arrows in $e^2fm^4$.

in the 82-126 shell ($2p_{1/2}$, $2p_{3/2}$, $1f_{5/2}$, $1f_{7/2}$, $0h_{9/2}$, and $0i_{13/2}$). The calculations are based on Kuo-Herling interaction [Herl79], which is an effective interaction tailored for this model space. The single-particle energies are those given by Warburton and Brown [Warb91]. In contrast to the results in Ref. [Koch17b] the ones in Fig. 1 are obtained with effective charges chosen to reproduce the measured $B(E2;8^+_1 \rightarrow 6^+_1)$ values for $^{210}$Pb and $^{210}$Po

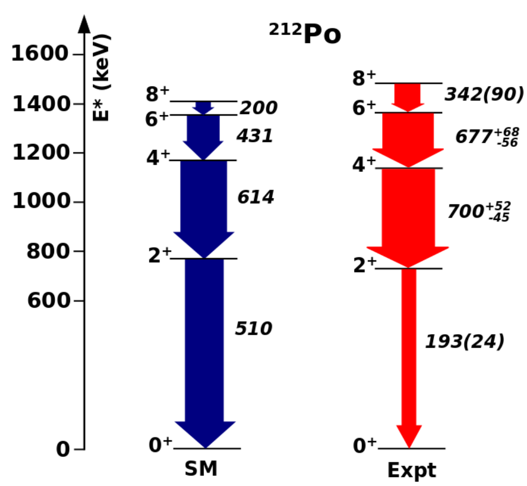


Figure 2: The same as Fig. 1 but for $^{212}$Po.

[Sham14] assuming that the $6^+_1$ and the $8^+_1$ states of these nuclei have pure two-nucleon configurations. This approach yields effective charges of $e_\nu = 0.91e$ and $e_\pi = 1.44e$.

The realistic shell model reproduces almost perfectly the energies of the yrast states in $^{210}$Pb and $^{210}$Po (cf. Fig. 1). However, the problem in the description of the $B(E2;2^+_1 \rightarrow 0^+_1)$ values is present for both nuclei – this value is clearly overestimated in $^{210}$Po and agrees

***only with the upper limit of the imprecise experimental value in $^{210}$Pb***. It has already been demonstrated that this problem cannot be resolved by tuning the effective charges [Koch17b] and that it is not specific for shell models only [Koch17a]. At the same time, the problem propagates in the description of open shell nuclei as can be seen in Fig. 2 where results from the same shell model for $^{212}$Po are presented. Apparently, the key for understanding the structure of the low-lying yrast states of nuclei north-east of $^{208}$Pb lies ***in the understanding of the behaviour of the seniority-2 configurations in $^{210}$Pb and $^{210}$Po.***

At this point there are two possible explanations about the discrepancy between the experimental and the shell model $B(E2;2^+_1 \rightarrow 0^+_1)$ values – either it is due to some deficiencies of the shell model as discussed in Refs. [Caur03, Koch17a, Kar19] or the experimental results for the lifetimes of the $2^+_1$ states of $^{210}$Pb [Elleg71] and $^{210}$Po [Koch17a] contain systematic errors. The latter option for $^{210}$Po has been put forward a few times recently [Gerat21, Stuch22]. Even though that no concrete evidence for such systematic errors in the result for the lifetime of the $2^+_1$ states of $^{210}$Po are found, the data evaluators for the A = 210 mass chain [Singh18] note that the $2^+$ lifetime measurement in $^{210}$Po should be tested by alternative methods. Indeed, accounting for the impact of the long-lived states feeding the level of interest always is a challenge in the DSA measurements and may shed doubts on the results for the obtained lifetimes. Coulomb excitation of radioactive ion beams is an experimental technique which is not affected by this problem and avoids any such criticism. ***Therefore, we propose to measure the $B(E2;2^+_1 \rightarrow 0^+_1)$ strengths in $^{210}$Po and $^{210}$Pb by the safe Coulomb excitation technique of radioactive ion beams.*** The study would be performed at ISOLDE in an off-line mode and will provide precise and reliable transition probabilities.

Another problem which also worth mentioning is the discrepancy between the theoretical and the experimental $B(E2;4^+_1 \rightarrow 2^+_1)$ values in $^{210}$Pb (cf. Fig. 1 and Ref. Koch17b). The lifetime of the $4^+_1$ state of $^{210}$Pb is, however, uncertain. The adopted value is $t_{1/2}$ = 0.6(1) ns, but there is an alternate experiment giving $t_{1/2}$ = 0.9(2) ns [Sham14]. The $4^+_1$ state of $^{210}$Pb can be populated in two-step Coulomb excitation. Under certain conditions the $B(E2;4^+_1 \rightarrow 2^+_1)$ can be determined with a higher precision. ***Providing that the necessary conditions can be achieved, we propose to attempt such a measurement as the secondary aim of the present proposal.***

## Required experimental conditions and yields

The ground-state lifetime of $^{210}$Po ($t_{1/2}$ = 138 d) will allow performing an experiment up to a few months after the production target has been irradiated by a proton beam, assuming the target is kept relatively "cold" during the irradiation in order to minimize any release of the products of interest. $^{210}$Po can be produced using a UCx target either directly or as a decay product through alpha-decay (from $^{226}$U) or beta decay (from $^{210}$At or $^{210}$Bi). From the different production paths it seems that the beta decay of $^{210}$At would provide the highest intensity, and, in the following estimations, we have considered only this option. Therefore, our estimates could be seen as a conservative lower limit values.

The ground-state lifetime of $^{210}$Pb ($t_{1/2}$ = 22 y) allows performing off-line experiments with it up to many years after the UCx target has been irradiated. $^{210}$Pb is produced through the alpha decay chain starting with $^{230}$U and $^{226}$Th. Uranium and thorium isotopes will not be released from the UCx target independent of the target temperature. The lifetime of $^{230}$U ($t_{1/2}$ = 21 d) means that the decay products, some of which are of a volatile character, would practically not be populated until the end of the irradiation period (usually 2 to 3 weeks). This means that $^{210}$Pb can be extracted from any of the "old" ISOLDE UCx targets from the last few years (i.e. there is no need to irradiate new target in order to perform an experiment with $^{210}$Pb).

In order to estimate the expected $^{210}$Po and $^{210}$Pb intensity on the Miniball target we discussed with the target-ion-source- [StorPR] the RILIS [MarsPR], the charge-breeding [WenaPR] and post-acceleration [RodrPR] experts at ISOLDE. The conservative in-target productions of $^{210}$Po and $^{210}$Pb could be estimated as $1\times10^8$ and $8\times10^7$ pps/μCi respectively. The laser ionization efficiencies are between 40% (for Po) and 30% (for Pb). The charge breeding efficiency was evaluated to be around 5% and 75% of post-acceleration efficiency was considered. Putting the numbers all together this gives between $1.5\times10^5$ and $2x10^5$ pps on the Miniball target. These estimates are rather conservative.

*Count rate estimates:*

We base the count rate estimates on an accelerated beam intensity delivered to Miniball of $2\times10^5$ pps. The best known $B(E2;2^+_1 \rightarrow 0^+_1)$ values [Elleg71, Koch17a] were used to calculate the Coulomb excitations cross-sections for $2^+_1$ states of $^{210}$Po and $^{210}$Pb. For calculating the Coulomb excitations cross-sections for $4^+_1$ state of $^{210}$Pb we used the $B(E2;4^+_1 \rightarrow 2^+_1)$ value reported in Ref. [Sham14]. The transition energies of interest are 1180 keV ($2^+_1 \rightarrow 0^+_1$ in $^{210}$Po), 800 keV ($2^+_1 \rightarrow 0^+_1$ in $^{210}$Pb), and 297 keV ($4^+_1 \rightarrow 2^+_1$ in $^{210}$Pb) for which we conservatively assume Miniball efficiencies of 5%, 8% and 16%, respectively. The beams of $^{210}$Po and $^{210}$Pb will be excited on a 2 mg/cm$^2$ thick $^{58}$Ni target. In order to ensure safe Coulomb excitation [Cline86] the beam energy is chosen to be 4.5 MeV/u.

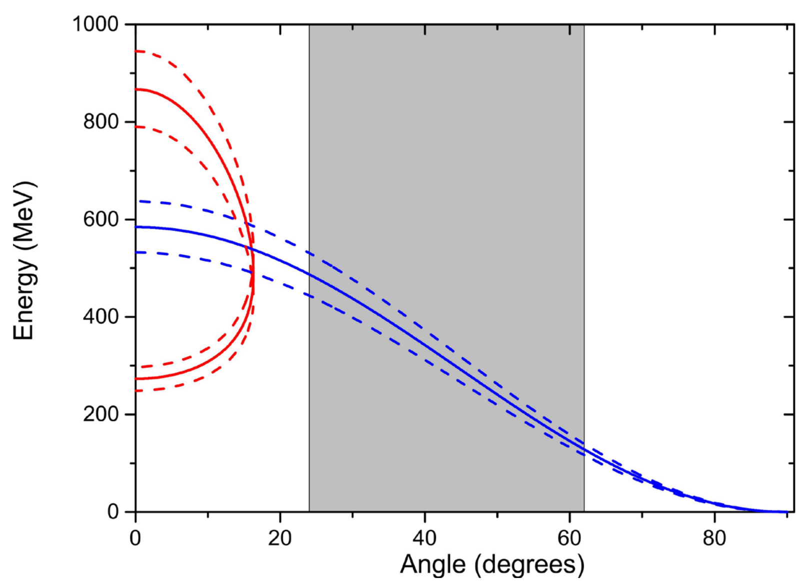


Figure 3: Reaction kinematics for 4.5 MeV/u $^{210}$Po/$^{210}$Pb (red) on 2 mg/cm$^2$ $^{58}$Ni target (blue). The shaded area indicates the angular coverage of the particle detector.

The proposed reaction is in inverse kinematics (cf. Fig. 3). The DSSD will placed 20 mm behind the target covering scattering angles between 24° and 62° in the laboratory system. As can be seen in Fig. 3 the beam ions will not scatter more than 16° which will prevent depositing any long-lived radioactivity on the DSSD.

Under these conditions it can be expected:

- ***912 gammas per day*** in the $2^+_1 \rightarrow 0^+_1$ in **$^{210}$Po** (3% statistical uncertainty).
- ***2352 gammas per day*** in the $2^+_1 \rightarrow 0^+_1$ in **$^{210}$Pb** (2% statistical uncertainty).
- ***55 gammas per day*** in the $4^+_1 \rightarrow 2^+_1$ in **$^{210}$Pb** (13% statistical uncertainty).

This statistics will allow for measuring the $B(E2;2^+_1 \rightarrow 0^+_1)$ values in $^{210}$Po and $^{210}$Pb with an uncertainty of better than 10%. If the beam intensities are higher than $2\times10^5$ pps on the Miniball target, the same level of precision can also be achieved for the $B(E2;4^+_1 \rightarrow 0^+_1)$ values in $^{210}$Pb.

## Summary of requested shifts:

- 3 shifts (1 day) with $^{58}$Ni target and $^{210}$Po beam at 4.5 MeV/u;
- 3 shifts (1 day) with $^{58}$Ni target and $^{210}$Pb beam at 4.5 MeV/u;
- 2 shifts for changing/tuning beams;
- 1 shift for calibrations;

## References:


[Caur03] E. Caurier, M. Rejmund, H. Grawe, Phys. Rev. C 67, 054310 (2003).

[Cline86] D. Cline Annu. Rev. Nucl. Part. Sci. 36, 683 (1986).

[Cor99] L. Coraggio *et al.*, Phys. Rev. C 60, 064306 (1999).

[Gerat21] M.S.M.Gerathy et al., Phys. Lett. B823, 136738 (2021).

[Goep50] Maria Goeppert Mayer, Phys. Rev. 78, 16 (1950).

[Elleg71] C. Ellegaard *et al.*, Nucl. Phys. A 162, 1 (1971).

[Elleg73] C. Ellegaard *et al.*, Nucl. Phys. A 206, 83 (1973).

[Häus76] O. Häusser *et al.*, Nucl. Phys. A 273, 253 (1976).

[Herl79] G. H. Herling and T. T. S. Kuo, Nucl. Phys. A 181, 113 (1979).

[Kar19] V. Karayonchev *et al.*, Phys. Rev. C 99 024326 (2019).

[Koch17a] D. Kocheva *et al.*, Eur. Phys. J. A 53, 175 (2017).

[Koch17b] D. Kocheva *et al.*, Phys. Rev. C 96, 044305 (2017)

[MarsPR] Bruce Marsh, private communication.

[RodrPR] Alberto Rodriguez, private communication.

[Sham14] M. Shamsuzzoha Basunia, Nucl. Data Sheets 121, 561 (2014).

[Shal63] A. de Shalit and I. Talmi, Nuclear Shell Theory (Academic Press, New York, 1963).

[Singh18] B. Singh, Experimental Unevaluated Nuclear Data List, 2018.

[StorPR] Thierry Stora and Simon Stegemann, private communication.

[Stuch22] A. E. Stuchbery and J. L. Wood, Physics 4, 697 (2022).

[Talm71] Igal Talmi, Nucl. Phys. A 172, 1 (1971).

[Warb91] E. K. Warburton and B. A. Brown, Phys. Rev. C 43, 602 (1991).
[WenaPR] Fredrik Wenander, private communication.

# Appendix

## DESCRIPTION OF THE PROPOSED EXPERIMENT

Please describe here below the main parts of your experimental set-up:

| Part of the experiment | Design and manufacturing |
|---|---|
| *If relevant, write here the name of the fixed installation you will be using*<br><br>Miniball + CD only | ☒ To be used without any modification<br><br>☐ To be modified |
| *If relevant, describe here the name of the flexible/transported equipment you will bring to CERN from your Institute*<br><br>[Part 1 of experiment/ equipment] | ☐ Standard equipment supplied by a manufacturer<br><br>☐ CERN/collaboration responsible for the design and/or manufacturing |
| [Part 2 experiment/ equipment] | ☐ Standard equipment supplied by a manufacturer<br><br>☐ CERN/collaboration responsible for the design and/or manufacturing |
| [insert lines if needed] | |

## HAZARDS GENERATED BY THE EXPERIMENT

Additional hazard from flexible or transported equipment to the CERN site:

| Domain | Hazards/Hazardous Activities | | Description |
|---|---|---|---|
| Mechanical Safety | Pressure | ☐ | [pressure] [bar], [volume][l] |
| | Vacuum | ☐ | |
| | Machine tools | ☐ | |
| | Mechanical energy (moving parts) | ☐ | |
| | Hot/Cold surfaces | ☐ | |
| Cryogenic Safety | Cryogenic fluid | ☐ | [fluid] [$m^3$] |
| Electrical Safety | Electrical equipment and installations | ☐ | [voltage] [V], [current] [A] |
| | High Voltage equipment | ☐ | [voltage] [V] |
| Chemical Safety | CMR (carcinogens, mutagens and toxic to reproduction) | ☐ | [fluid], [quantity] |
| | Toxic/Irritant | ☐ | [fluid], [quantity] |
| | Corrosive | ☐ | [fluid], [quantity] |
| | Oxidizing | ☐ | [fluid], [quantity] |

| | | | |
|---|---|---|---|
| | Flammable/Potentially explosive atmospheres | ☐ | [fluid], [quantity] |
| | Dangerous for the environment | ☐ | [fluid], [quantity] |
| **Non-ionizing radiation Safety** | Laser | ☐ | [laser], [class] |
| | UV light | ☐ | |
| | Magnetic field | ☐ | [magnetic field] [T] |
| **Workplace** | Excessive noise | ☐ | |
| | Working outside normal working hours | ☐ | |
| | Working at height (climbing platforms, etc.) | ☐ | |
| | Outdoor activities | ☐ | |
| **Fire Safety** | Ignition sources | ☐ | |
| | Combustible Materials | ☐ | |
| | Hot Work (e.g. welding, grinding) | ☐ | |
| **Other hazards** | | | |
| | | | |